Acquired phototrophy stabilizes coexistence and shapes intrinsic dynamics of an intraguild predator and its prey

December 10, 2015

Holly V. Moeller[1,†], Elina Peltomaa[2], Matthew D. Johnson[1,3], and Michael G. Neubert[1,4]

[1]Department of Biology, Woods Hole Oceanographic Institution, Woods Hole, MA, USA.

[2]Department of Environmental Sciences, University of Helsinki, Helsinki, Finland. elina.peltomaa@helsinki.fi.

[3]mneubert@whoi.edu.

[4]mattjohnson@whoi.edu.

[†]Corresponding Author. 266 Woods Hole Road, Mail Stop 52, Woods Hole, MA 02543. holly@whoi.edu. +1 508 289-3819.

Author Contributions: HVM and MGN wrote the model. HVM analyzed the model and designed the validation experiments. HVM and EP conducted the experiments and analyzed the data. All authors wrote the paper.

Running Title: Acquired phototrophy in plankton communities

Keywords: acquired metabolic potential, community ecology, intraguild predation, kleptoplastidy, *Mesodinium rubrum*, mixotrophy

Article Type: Letter

Abstract: 150 words; Main Text: 3356 words; 44 References; 1 Table; 5 Figures

Abstract

In marine ecosystems, acquired phototrophs—organisms that obtain their photosynthetic ability by hosting endosymbionts or stealing plastids from their prey—are omnipresent. Such taxa function as intraguild predators yet depend on their prey to periodically obtain chloroplasts. We present new theory for the effects of acquired phototrophy on community dynamics by analyzing a mathematical model of this predator-prey interaction and experimentally verifying its predictions with a laboratory model system. We show that acquired phototrophy stabilizes coexistence, but that the nature of this coexistence exhibits a 'paradox of enrichment:' as light increases, the coexistence between the acquired phototroph and its prey transitions from a stable equilibrium to boom-bust cycles whose amplitude increases with light availability. In contrast, heterotrophs and mixotrophic acquired phototrophs (that obtain <30% of their carbon from photosynthesis) do not exhibit such cycles. This prediction matches field observations, in which only strict (>95% of carbon from photosynthesis) acquired phototrophs form blooms.

Introduction

An organism's interaction with its environment is fundamentally mediated by its metabolic potential—its ability to incorporate and chemically transform a suite of substrates to fuel its growth and reproduction. Especially in microbial communities, the scope of an organism's metabolic potential determines its fundamental niche, while the efficiency of its metabolism compared to competing species determines its realized niche (McGill *et al.*, 2006). Some organisms are capable of extending their metabolic niche through the acquisition of metabolic potential: During their lifetimes, they acquire genes (Ochman *et al.*, 2000; Falkowski & Fenchel, 2008) and/or cellular machinery (Stoecker *et al.*, 2009; Johnson, 2011; Park *et al.*, 2014) from other species that allow them to perform metabolic reactions not otherwise coded in their own genomes. These acquisitions have been highly ecologically and evolutionarily successful. For example, many marine planktonic protists contain photosynthetic machinery acquired from their prey (Stoecker *et al.*, 1987) and, as a consequence, can be major contributors to local primary production (Stoecker *et al.*, 1989), including through the formation of planktonic blooms (Yih *et al.*, 2013; Crawford *et al.*, 1997). Further, endosymbiosis theory postulates that plastids evolved from free-living cells whose metabolism was acquired when they were engulfed by their hosts (Sagan, 1967).

Acquired metabolism may shape community dynamics by altering interspecific interactions such as competition. For example, acquired phototrophy, in which an organism acquires photosynthesis by hosting either endosymbiotic phototrophs or their organelles (Johnson, 2011), transforms otherwise heterotrophic taxa into mixotrophs. Especially in planktonic microbial communities, protistan acquired phototrophs may function similarly to intraguild predators, both competing with and consuming the algal prey from which they steal chloroplasts.

Unlike traditional intraguild predators, however, an acquired phototroph's competitive ability (for light, via photosynthesis) is fundamentally reliant on the persistence of its competitor (from which it must periodically acquire cellular machinery). In principle, this dependence may produce qualitatively different community dynamics than those ob-

served in either simple competition or intraguild predation scenarios. Theory predicts that, when two species compete directly for a common resource, only the species capable of persisting at the lowest availability level of that resource (i.e., the species with the lowest R^*) should persist at equilibrium (Tilman, 1977; Huisman & Weissing, 1994). Intraguild predation may modify this outcome, particularly when the inferior competitor predates the other species (Polis & Holt, 1992). However, the effects of acquired metabolism—and, in particular, acquired phototrophy—on species competition and coexistence remain, as yet, relatively unknown.

Here, we present new theory, which we compare with laboratory and field data, that describes the coexistence of acquired phototrophs and their prey and predicts how competitive outcomes differ depending upon environmental conditions. We modified a classical model of phytoplankton competition (Huisman & Weissing, 1994) to account for the acquisition of photosynthesis by one species and analyzed outcomes of species interactions. We compared the model's qualitative predictions with an experimentally manipulated laboratory model of acquired phototrophy: the marine ciliate *Mesodinium rubrum* (Lohmann 1908) and the cryptophyte alga *Geminigera cryophila* (Taylor & Lee, Hill 1991) from which it acquires its photosynthetic machinery. *M. rubrum* is a globally distributed bloom-former in coastal and estuarine systems that may be responsible for up to 90% of microplankton primary production (Stoecker *et al.*, 1989). Data from *M. rubrum* blooms suggest that it is a specialist predator: its acquired plastids come from a single algal species though the exact identity of that species depends upon geographic location (Hansen *et al.*, 2013; Herfort *et al.*, 2011; Gustafson *et al.*, 2000; Smith & Hansen, 2007). Finally, we used our model to generate predictions of annual community dynamics for consumers with different degrees of reliance on acquired heterotrophy, and linked these predictions with field observations of planktonic communities to determine the applicability of this theory to real-world systems.

Methods

The Model

To study the effects of acquired phototrophy on community dynamics, we developed a model of two interacting planktonic species that reside in a well-mixed water column (i.e., each cell experiences the same average light intensity, Figure S1) by modifying Huisman and Weissing's (1994) classic model for phytoplankton competition, in which two species compete for light.

The net growth rate at depth z of each phytoplankter is governed by the balance between its photosynthetic rate (p_i, which depends on the local irradiance I) and its carbon loss rate (l_i):

$$g_i(z) = p_i(I(z)) - l_i = p_{\max,i}\ \frac{I(z)}{H_i + I(z)} - l_i. \tag{1}$$

Here, $p_{\max,i}$ is the species' maximum photosynthetic rate, H_i is the irradiance at which cells photosynthesize at half that rate, and l_i is the per cell loss rate. For persistence of the phytoplankter, $p_{\max,i}$ must be greater than l_i. In a homogeneous water column, $I(z)$ depends upon incident (surface) light I_{in}, the absorptivity k_i of each of the phytoplankton cells, and the density of the phytoplankton cells w_i, according to the Lambert-Beer law:

$$I(z) = I_{\text{in}} e^{-(k_1 w_1 + k_2 w_2)z} \tag{2}$$

(Figure S1).

Integrating net growth $g_i(z)$ over the water column, the rate of change in abundance of each of the phytoplankton populations (W_i) is given by:

$$\frac{dW_i}{dt} \;=\; \frac{p_{max,i} W_i}{\sum_i k_i W_i} \ln\left[\frac{H_i + I_{\text{in}}}{H_i + I_{\text{in}} \exp(-\sum_i k_i W_i)}\right] - l_i W_i \tag{3}$$

(see Huisman & Weissing (1994) for details).

Using this model, Huisman & Weissing (1994) showed that competitive exclusion

should occur except for special parameter combinations that produce functionally identical species. Because the two species are competing for a shared resource, only the species able to grow at the lowest light level (I^*, analogous to R^*, *sensu* Tilman (1977)) persists at equilibrium.

To test the robustness of this conclusion to acquired phototrophy, we introduced stage structure for one of the two competing species (Figure 1a, Table 1). In particular, we assumed that this second species is a consumer that exists in one of two states: C_H, a heterotrophic state in which it grows through direct incorporation of prey carbon into its biomass; and C_P, an autotrophic state in which it grows through photosynthetic fixation of carbon. Only the heterotrophic state predates the phytoplankter. We assumed a Type I functional response (Holling, 1959) with an attack rate a. Such a linear response of predation pressure to prey concentration is reasonable for the low prey abundances and high consumer clearance rates typical of many planktonic systems, and has been empirically observed in acquired phototrophs (e.g., Hansen *et al.*, 2004).

A fraction f of predation events lead to acquired phototrophy (i.e., sequestration of phytoplankton cellular machinery such as chloroplasts), transforming the consumer from state C_H to state C_P. The rest $(1 - f)$ of the predation events lead to heterotrophic growth with a phytoplankter-to-consumer conversion efficiency e. We further assumed that acquired photosynthetic machinery cannot be retained indefinitely by the consumer. Thus, plastids are lost at a rate m, inducing a transition from state C_P to state C_H. We also assumed that the consumer cannot independently replicate photosynthetic equipment, so photosynthesis by the phototrophic state C_P produces additional heterotrophic consumers C_H. This formulation, therefore, is more representative of kleptoplastidic acquired phototrophs than those that harbor endosymbionts, because the latter may be able to vertically transmit acquired phototrophy when the cells they host divide (Stoecker *et al.*, 2009).

The mathematical representation of this model is:

$$\frac{dW}{dt} = \frac{p_W W}{\kappa} \ln\left[\frac{H_W + I_{\text{in}}}{H_W + I_{\text{in}} \exp(-\kappa)}\right] - l_W W - aWC_H \quad (4)$$

$$\frac{dC_H}{dt} = \frac{p_P C_P}{\kappa} \ln\left[\frac{H_P + I_{\text{in}}}{H_P + I_{\text{in}} \exp(-\kappa)}\right] - C_H\left[l_H + afW - a(1-f)eW\right] + mC_P \quad (5)$$

$$\frac{dC_P}{dt} = afWC_H - l_P C_P - mC_P \quad (6)$$

where $\kappa = k_W W + k_H C_H + k_P C_P$.

This formulation allows us to tune the model to represent different consumer functional types, from strict acquired phototrophs, which obtain all of their carbon from photosynthesis (Figure 1b; $f = 1$), to strict heterotrophs, which obtain all of their carbon from heterotrophy and do not retain prey plastids (Figure 1c; $f = 0$).

We used a combination of analytical approaches and numerical simulations to identify types of community dynamics (i.e., stable equilibrium points with one or both species, and stable limit cycles) and determine the boundaries between them in parameter space. We only considered cases for which W is a superior competitor (e.g., has a higher $p_{\max}$, lower H, lower k, or lower l than the consumer) and, in the purely competitive system (eq. 3), would exclude the consumer. We based this assumption on our reasoning that photosynthetic equipment operates most efficiently in its native host (e.g., van den Hoff & Bell 2015), which was confirmed by our empirical observations reported below. We also assumed that consumers experience higher intrinsic mortality in the heterotrophic state compared to the phototrophic state. Because our model does not consider higher trophic level predators, this assumption is based on the intuition that, without photosynthetic equipment to fix carbon, the consumer is less likely to be able to meet its basal energetic needs and thus experiences higher mortality. This reasoning is supported by experimental data on the mortality rates of starved acquired phototrophs (Crawford & Stoecker, 1996; Schoener & McManus, 2012; Skovgaard, 1998).

We began our analysis by assuming strict acquired phototrophy (i.e., $f = 1$). We studied the dependence of model dynamics on input light (I_{in}), species interaction strength

Table 1: Model symbols and their meanings

Symbol	Description	Typical Units	Value for Simulations	Value for Empirical Comparisons
Variables:				
W	phytoplankton, prey species	cells		
C_H	consumer, heterotrophic state	cells		
C_P	consumer, phototrophic state	cells		
t	time	days		
Parameters:				
I_{in}	Light intensity at top of water column	μmol quanta m^{-2} s^{-1}	variable	0.5, 5, 50
p_W	maximum photosynthetic rate, phytoplankter	day^{-1}	3	0.5
p_P	maximum photosynthetic rate, consumer	day^{-1}	2	0.2
k_W	light absorbance of W	cell^{-1}	0.1	0.00001
k_H	light absorbance of C_H	cell^{-1}	0.05	0.000005
k_P	light absorbance of C_P	cell^{-1}	0.15	0.000015
H_W	half-saturation light intensity for W	μmol quanta m^{-2} s^{-1}	10	0.5
H_P	half-saturation light intensity for C_P	μmol quanta m^{-2} s^{-1}	10	10
l_W	mortality rate of W	day^{-1}	0.5	0.2
l_H	mortality rate of C_H	day^{-1}	0.5	0.03
l_P	mortality rate of C_P	day^{-1}	0.1	0.01
a	attack rate of C_H on W	day^{-1} cell^{-1}	variable	0.000032
f	fraction of predation events leading to acquisition	–	variable	1
e	heterotrophic conversion efficiency of W to C_H	cell cell^{-1}	0.1	n/a
m	plastid loss rate	day^{-1}	variable	0.1
I_{mean}	mean incident irradiance when light varies over time	μmol quanta m^{-2} s^{-1}	50	n/a
I_{var}	degree of seasonal variation in incident light	–	0.9	n/a

(represented by the attack rate a), and mean plastid retention time ($1/m$). For each value of a and m, we determined three input light thresholds that demarcate types of model dynamics. The first threshold is I_C, the compensatory irradiance for W (above which its net growth rate is positive), which can be determined analytically as $l_W H_W/(p_W - l_W)$ (Huisman & Weissing 1994). The second, I_{COEX}, is the irradiance above which the consumer can persist alongside W in the system. Finally, I_{LC} is the irradiance above which the coexistence attractor takes the form of a limit cycle rather than an equilibrium point.

Empirical model validation using a strict acquired phototroph

We tested our model's applicability to planktonic community dynamics by comparing its qualitative predictions for a strict acquired phototroph ($f = 1$) to the dynamics of a laboratory model acquired phototroph, *Mesodinium rubrum* (CCMP 2563), and its cryptophyte alga prey, *Geminigera cryophila* (CCMP 2564). *M. rubrum* is a strict acquired phototroph: it obtains ∼98% of its carbon from photosynthesis using plastids stolen from *G. cryophila* (Hansen *et al.*, 2013; Johnson & Stoecker, 2005). However, it must periodically feed on *G. cryophila* to re-acquire the prey nuclei that it uses to run these chloroplasts (Johnson *et al.*, 2007). Absent prey, *M. rubrum* loses its nuclei, followed by loss of its photosynthetic abilities and, finally, cell death. Thus, like our mathematical model's consumer, *M. rubrum* exhibits two states: one in which it grows and divides photosynthetically, and one in which its growth stalls while it seeks to acquire prey machinery through predation.

Because both species were initially isolated from McMurdo Sound, Antarctica, we mimicked summer, high-latitude conditions by incubating cultures at low temperature (4°C), and constant (24-hour) low light (0.5, 5, or 50 μmol quanta m^{-2} $s^{-}1$). Based on prior knowledge of the compensation (0.7 μmol quanta m^{-2} s^{1}) and saturation (20 μmol quanta m^{-2} s^{-1}) irradiances for *M. rubrum* growth (Moeller *et al.*, 2011), we expected these three light levels to result in phytoplankter-only, stable coexistence, and limit cycle dynamics, respectively. We used a batch-culture method to test this hypothesis. Specifically, we set up two replicate flasks of 35 PSU f/2-Si media (Guillard, 1975) at each of

the three light levels (except 0.5 μmol quanta m^{-2} s^{-1}, which had only one replicate), and inoculated them with *M. rubrum* cultures that had been allowed to acclimate to the respective light levels for a period of three months, with their most recent *G. cryophila* feeding two months previous to the start of the experiment. Approximately every three days for the fifty-day experimental period, we fixed a 1.25mL sample of each culture with 1% Lugol's Iodine, and enumerated both consumer and prey cells using a compound light microscope at 100x (oculars + objective) magnification. Nutrients were not replenished during the course of the experiment; the fifty-day experimental period was chosen so that the experiment was halted before cultures exhibited population declines characteristic of nutrient limitation.

At the experimental start point, cultures differed in their ratio of prey to acquired phototrophs because of their light incubation and feeding history. Specifically, high-light incubations had very low prey densities (because of grazing by *M. rubrum* subsequent to the last previous feeding, two months prior), whereas low-light incubations had higher ratios (due to relatively higher prey growth rates). Therefore, to produce comparable mathematical model simulations for the *M. rubrum*-*G. cryophila* system, we used published data (Johnson *et al.*, 2006; Moeller *et al.*, 2011) to identify the appropriate ranges for parameter values (Table 1), and then adjusted parameters manually to maximize agreement with the data. We set the model's initial conditions according to starting experimental data. We then calculated the ratio of prey to acquired phototrophs over time for both types of data. (Using ratios allowed us to normalize for dilutions, incomplete flask homogenization before sampling, and other sources of experimental noise.) We pooled our log-transformed experimental ratios by light level and fit two types of models to these data: (1) a linear model, and (2) a piecewise linear model with a single breakpoint (using the R (version 3.1.0, R Core Team 2014) package *segmented*, Muggeo 2003). To select the best-fitting statistical model, we first used an analysis of variance (ANOVA) test to determine whether the models were significantly different. If they were not, we selected the linear model based on parsimony; if they were, we defined the best-fitting model as the model with the lowest Akaike information criterion (AIC) score.

Varying reliance on acquired phototrophy

Marine planktonic communities also include acquired phototrophs that rely less on photosynthesis for their carbon supply (Stoecker *et al.*, 2009; Johnson, 2011). We therefore relaxed our assumption of strict acquired phototrophy and allowed for a range of degrees of dependence on photosynthesis as a carbon source. Among acquired phototrophs, the retention time of acquired machinery is correlated with dependence on photosynthesis: strict acquired phototrophs such as *M. rubrum* retain prey nuclei with a half-life of ten days and retain plastids indefinitely, whereas some mixotrophic oligotrich ciliates retain plastids for as little as a few hours (Stoecker *et al.*, 2009; Johnson, 2011). Therefore, we set $m = 3 - 2.9f$, which represents a linear interpolation between *M. rubrum*, for which $f = 1$ and $m = 0.1$, and a strict heterotroph, for which $f = 0$ and clearance rates are on the order of hours ($m = 3$). We determined the dependence of the irradiance thresholds I_C, I_{COEX}, and I_{LC} on f and m.

Finally, we used our model to predict seasonal dynamics of planktonic communities whose members exhibit varying degrees of reliance on acquired phototrophy. The incident light received by the surface ocean varies seasonally. Therefore, we varied I_{in} over time using

$$I_{\text{in}}(t) = I_{\text{mean}} \left[1 + I_{\text{var}} \sin\left(\frac{2\pi t}{365} \right) \right], \tag{7}$$

where I_{mean} is the mean annual surface irradiance and I_{var} is the degree of seasonal variation (from 0 to 1). Because time is measured in days, $I_{\text{in}}(t)$ has a period of one year.

We simulated population dynamics for four scenarios: (1) phytoplankter only, (2) phytoplankter and strict acquired phototroph ($f = 1$, $m = 0.1$), (3) phytoplankter and mixotrophic acquired phototroph ($f = 0.3$, $m = 2$), and (4) phytoplankter and strict heterotroph ($f = 0$, $m = 10$). We compared our findings with field observations of planktonic community dynamics, with special attention to contrasting life histories among bloom-forming and non-bloom-forming consumers.

Results

Dynamics of strict acquired phototrophy

To qualitatively explore the dynamics exhibited by our model, we first considered the case of a strict acquired phototroph which is dependent upon acquired photosynthetic equipment for growth (Figure 1b). In this case, f, the fraction of predation events that leads to plastid acquisition, is 1; other parameter values are given in Table 1.

The model exhibits four different types of dynamics as surface irradiance I_{in} is intensified (Figure 2). When I_{in} is below the minimum light requirement for phytoplankton growth (I_C), neither phytoplankter nor consumer persist, and the equilibrium $(W, C_H, C_P) = (0, 0, 0)$ is stable. When I_{in} is greater than I_C but less than I_{COEX}, $(W, C_H, C_P) = (W^*, 0, 0)$ is the only stable equilibrium: only the phytoplankter persists. If I_{in} exceeds the boundary for coexistence I_{COEX}, the phytoplankter and consumer coexist. For $I_{COEX} < I_{\text{in}} < I_{LC}$, this coexistence occurs at a stable equilibrium point: the population sizes of the phytoplankter and both consumer stages are asymptotically constant over time. However, once I_{in} exceeds I_{LC}, this equilibrium point becomes unstable and the population dynamics converge on a limit cycle. These limit cycles increase in amplitude with increasing light intensity, with corresponding decreases in minimum population sizes for both phytoplankter and consumer (Figure S2).

Increasing either the attack rate a (Figure 2a) or the plastid retention time $1/m$ (Figure 2b) reduces the minimum irradiance for coexistence. Increasing these parameters also increases the range of light levels at which limit cycles are present. Note that, because the consumer is dependent upon the phytoplankter for its acquired metabolism, the phytoplankter is never eliminated from the system, but rather (in the case of limit cycles) recovers in population size after the consumer population crashes.

Comparison with empirical data

Our observations of population dynamics of the strict acquired phototroph *Mesodinium rubrum* and its cryptophyte phytoplankter prey *Geminigera cryophila* were qualitatively

consistent with model predictions (Figures 3, S3). We observed three qualitatively different types of community dynamics. At the lowest light level, which was below the compensation irradiance for *M. rubrum* growth (Moeller *et al.*, 2011), only *G. cryophila* exhibited positive growth, and the ratio of prey to consumers grew exponentially (best fit to data: linear model without breakpoint; $P < 0.001$, $R^2 = 0.928$). At the intermediate light level, *G. cryophila* and *M. rubrum* populations stabilized at a fixed prey to consumer ratio (best fit to data: single breakpoint at 29.4 days with change from positive to zero slope; $P < 0.001$, $R^2 = 0.976$). Finally, at the highest light level, a population boom of *G. cryophila* was curtailed and then outpaced by growth of *M. rubrum*, leading to an increase, then decrease in the ratio of prey to consumers (best fit to data: single breakpoint at 21.4 days with change from positive to negative slope; $P < 0.001$, $R^2 = 0.896$). Accounting for the effects of photoacclimation by allowing H_W, the half-saturation light intensity for phytoplankter growth, to vary with irradiance improved the model's quantitative fit (Table S1, Figure S4).

Dynamics along the mixotrophy spectrum

The model predicts that the extent of the consumer's reliance on acquired phototrophy (examples from across the heterotrophy-autotrophy gradient are given along the abscissa in Figure 4a and pictured in Figure 4b-f) has major qualitative effects on community dynamics (Figure 4a; see Figure S5 for f varied in isolation). Strict acquired phototrophs exhibit cyclic dynamics, even at low irradiance levels, whereas strict heterotrophs exhibit time-invariant stable population sizes. To test whether the absence of cyclic dynamics was a result of our choice of Type I predator functional response, we modified the model to include a Type II functional response. Type II functional responses, which account for predator handling time and are thought to be common in natural systems, can give rise to cyclic dynamics. However, in our case we found that even when we varied handling time over several orders of magnitude, the model's asymptotic behavior did not change indicating that dynamics were not sensitive to our choice of functional response.

This difference in intrinsic dynamics (i.e., presence or absence of limit cycles) drives

differences in annual community dynamics when light varies seasonally (Figure 5). While the presence of any consumer curtails the extent of the phytoplankton bloom (compare peaks in Figure 5 panel b to panels c-e), only communities with strict acquired phototrophs (Figure 5c, $f = 1$, $m = 0.1$) exhibit sequential blooms in which a boom and then crash in the phytoplankton population is followed by the consumer's own boom-bust cycle. In contrast, mixotrophic acquired phototrophs, which grow on a combination of photosynthetic and heterotrophic carbon sources (Figure 5d), and strict heterotrophs (Figure 5e) track phytoplankton biomass.

Discussion

Acquired phototrophs, organisms which rely on photosynthetic endosymbionts or their plastids to conduct photosynthesis, are omnipresent in planktonic communities where they function, to varying degrees, as heterotrophic predators and phototrophic competitors (Stoecker *et al.*, 1987). The results of our analysis show that acquired phototrophy can stabilize coexistence by allowing an otherwise weaker competitor to act as an intraguild predator that nonetheless requires the persistence of its prey for periodic metabolic acquisition. Thus acquired metabolic potential may be another mechanism which helps to explain the so-called 'paradox of the plankton' (Hutchinson, 1961).

Because of their dual function as predator and competitor, acquired phototrophs may drive cyclic community dynamics with sequential booms and crashes of phytoplankton prey and acquired phototrophs. When we incorporated seasonal variation in light availability, strict acquired phototrophs, which rely entirely on photosynthesis for growth, exhibited "bloom" dynamics, with population sizes increasing 100-fold following the cessation of prey blooms. Indeed, when we surveyed the literature for species whose physiologies spanned the range of reliance on acquired phototrophy (Figure 4a, colored bars), we found that only the strict acquired phototroph end members (*M. rubrum* and green *Noctiluca scintillans*) are known bloom-formers (Hansen, 2011). In contrast, the mixotrophic acquired phototrophs are common but low-density community members whose abundance

tends to track phytoplankton abundance (Löder *et al.*, 2011; Nielsen & Kicrboe, 1994). Published time series data which include heterotrophic and acquired phototroph mesozooplankton suggest that strict acquired phototrophs (e.g., *M. rubrum*) exhibit more pronounced "blooms" than the low-abundance oligotrich ciliates, which in turn exhibit larger population swings than strict heterotrophs (Löder *et al.*, 2011; Ribera d'Alcala *et al.*, 2004; Lessard & Murrell, 1996).

Comparisons between our model's predictions and field observations are suggestive of the intrinsic importance of acquired phototrophy to community dynamics. However, marine planktonic communities are far more complex than our simple two-species model, which does not account for top-down controls such as zooplankton grazing, other forms of bottom-up constraints such as nutrient supply, or the presence of other phytoplankton and mesozooplankton competitors. Indeed, the model also ignores biological nuances of the focal species themselves, such as photoacclimation, which affects photosynthetic rates and carbon budgets at different light levels (Moeller *et al.*, 2011; Skovgaard, 1998; Nielsen *et al.*, 2012), motility, which may allow acquired phototrophs to reach nutrient supplies at the boundary of the mixed layer (Stoecker *et al.*, 1989), and light-dependence of pure heterotrophs, whose grazing and digestion rates increase with light availability (Strom, 2001).

Nonetheless, our model qualitatively predicted the light-dependence of the dynamics of the laboratory model *M. rubrum*-*G. cryophila* system, identifying a sequence of transitions with increasing light from a single-species equilibrium to a coexistence equilibrium to cyclic dynamics. There are several possible explanations for quantitative discrepancies between our mathematical and laboratory model systems. First, because the experimental observations lasted for only fifty days (after which, at high light levels, both species declined, likely due to nutrient limitation), we were unable to observe long-term population dynamics. Second, while we used a single set of biological parameters and three different irradiance levels to generate our simulation data, in reality many of the biological parameters are light-dependent. For example, photoacclimation allows both prey and consumer to adjust growth and respiration rates to light availability (Moeller *et al.*,

2011; Johnson *et al.*, 2006). Additionally, attack and prey processing rates may be light dependent (Strom, 2001). Furthermore, differences in feeding history driven by light-dependent dynamics in the acclimation period prior to the experiment may have further altered biological rates (Johnson *et al.*, 2006). However, our experiment did confirm the importance of light availability to qualitative model dynamics.

In both our model and our laboratory system, increasing the light supply destabilized the equilibrium coexistence point in favor of limit cycles. The amplitude of modeled limit cycles increased with increasing surface irradiance, with population sizes periodically falling to very low levels which, in real-world systems, could lead to local extinction. Thus our model suggests that acquired phototrophy may produce another example of the 'paradox of enrichment,' in which an increased carrying capacity (here, increased light) destabilizes population dynamics (Rosenzweig, 1971). Empirical studies have shown that increasing light levels can also increase grazing and digestion rates (Nielsen *et al.*, 2012; Skovgaard, 1998; Feinstein *et al.*, 2002; Park *et al.*, 2014), and increase the degradation rate of plastids through photooxidative stress (Johnson & Stoecker, 2005). These mechanisms, while not explicitly included in our model, may further destabilize equilibrium points in natural systems.

With the exception of strict acquired phototrophs and strict heterotrophs (which get 100 and 0% of their carbon from photosynthesis, respectively), the organisms we modeled are part of the broad class of microplankton known as mixotrophs, which combine heterotrophy and phototrophy for growth. Here, we have focused explicitly on acquired phototrophy as the mechanism through which our consumers access photosynthesis and considered only competition for light. However, others have studied the more general role of mixotrophy on community composition and stability with particular attention to competition for other resources, such as nutrients (e.g., Stickney *et al.*, 1999; Crane & Grover, 2010; Flynn & Mitra, 2009; Mitra & Flynn, 2010). This work has underscored the importance of determining the extent to which mixotrophs rely on their different nutritional modes (Flynn & Mitra, 2009; Mitra & Flynn, 2010). Typically, the persistence of mixotrophs (e.g., in a water column that may also contain phototrophs, heterotrophs,

remineralizing bacteria and higher trophic level consumers) hinges upon their ability to supplement their carbon budget with photosynthesis under low-prey conditions, or their nutrient budget with heterotrophy under low-nutrient conditions (Crane & Grover, 2010). Low levels of mixotroph grazing have also been shown to induce population oscillations (Stickney *et al.*, 1999), though not to the extent of the limit cycles present in our model's parameter space.

In conclusion, our results, in the context of field observations, highlight the importance of acquired phototrophy as a driver of community dynamics. As both heterotrophic and phototrophic members of the microplankton, marine acquired phototrophs play a key role in modulating the primary production that underlies the larger marine food web (Stoecker *et al.*, 1989, 2009; Mitra *et al.*, 2013). However, acquired phototrophs are just one example of acquired metabolic potential, a phenomenon that raises evolutionary, as well as ecological, questions about selective constraints on an organism's niche and the process of endosymbiosis (Keeling *et al.*, 2015). That organisms utilizing metabolism not encoded in their own genomes can have such a profound impact on community dynamics highlights their importance and the need for additional theoretical and empirical studies of their ecology.

Acknowledgements

The authors thank Christopher Kirby for assistance in the lab. Hal Caswell, Po-Ju Ke, Emily Moberg, Sandeep Venkataram, and Naupaka Zimmerman provided valuable feedback and discussion. HVM is supported by a United States National Science Foundation Postdoctoral Research Fellowship in Biology (Grant No. DBI-1401332). EP is supported by the Academy of Finland through research grant 276268. MDJ acknowledges NSF Grant No. IOS-1354773. MGN acknowledges support provided by the Independent Research and Development Program at the Woods Hole Oceanographic Institution.

References

Crane, K. W. & Grover, J. P. (2010). Coexistence of mixotrophs, autotrophs, and heterotrophs in planktonic microbial communities. *Journal of Theoretical Biology*, 262, 517–527.

Crawford, D. W., Purdie, D. A. & Lockwood, A. (1997). Recurrent red-tides in the Southampton water estuary caused by the phototrophic ciliate *Mesodinium rubrum*. *Estuarine, Coastal and Shelf Science*, 45, 799–812.

Crawford, D. W. & Stoecker, D. K. (1996). Carbon content, dark respiration and mortality of the mixotrophic planktonic ciliate *Strombidium capitatum*. *Marine Biology*, 126, 415–422.

Falkowski, P. & Fenchel, T. (2008). The microbial engines that drive Earth's biogeochemical cycles. *Science*, 320, 1034–1039.

Feinstein, T. N., Traslavina, R., Sun, M. Y. & Lin, S. (2002). Effects of light on photosynthesis, grazing, and population dynamics of the heterotrophic dinoflagellate *Pfiesteria piscicida* (Dinophyceae). *Journal of Phycology*, 38, 659–669.

Flynn, K. J. & Mitra, A. (2009). Building the "perfect beast": modelling mixotrophic plankton. *Journal of Plankton Research*, 31, 965–992.

Guillard, R. R. L. (1975). Culture of phytoplankton for feeding marine invertebrates. In: *Culture of Marine Invertebrate Animals* (eds. Smith, W. L. & Chanley, M. H.). Plenum Press, New York, pp. 26–60.

Gustafson, D., Stoecker, D., Johnson, M. & Van, W. (2000). Cryptophyte algae are robbed of their organelles by the marine ciliate *Mesodinium rubrum*. *Nature*, 405, 1049–1052.

Hansen, P. J. (2011). The role of photosynthesis and food uptake for the growth of marine mixotrophic dinoflagellates. *Journal of Eukaryotic Microbiology*, 58, 203–214.

414 Hansen, P. J., Miranda, L. & Azanza, R. (2004). Green *Noctiluca scintillans*: a dinoflagellate with its own greenhouse. *Marine Ecology Progress Series*, 275, 79–87.

416 Hansen, P. J., Nielsen, L. T., Johnson, M., Berge, T. & Flynn, K. J. (2013). Acquired phototrophy in *Mesodinium* and *Dinophysis* – A review of cellular organization, prey 418 selectivity, nutrient uptake and bioenergetics. *Harmful Algae*, 28, 126–139.

Herfort, L., Peterson, T. D., Campbell, V., Futrell, S. & Zuber, P. (2011). *Myrionecta* 420 *rubra* (*Mesodinium rubrum*) bloom initiation in the Columbia River estuary. *Estuarine, Coastal and Shelf Science*, 95, 440–446.

422 Holling, C. S. (1959). Some characteristics of simple types of predation and parasitism. *The Canadian Entomologist*, 91, 385–398.

424 Huisman, J. & Weissing, F. J. (1994). Light-limited growth and competition for light in well-mixed aquatic environments: an elementary model. *Ecology*, 75, 507–520.

426 Hutchinson, G. E. (1961). The paradox of the plankton. *The American Naturalist*, 95, 137–145.

428 Johnson, M., Oldach, D., Delwiche, C. & Stoecker, D. (2007). Retention of transcriptionally active cryptophyte nuclei by the ciliate *Myrionecta rubra*. *Nature*, 445, 426–428.

430 Johnson, M. & Stoecker, D. (2005). Role of feeding in growth and photophysiology of *Myrionecta rubra*. *Aquatic Microbial Ecology*, 39, 303–312.

432 Johnson, M. D. (2011). The acquisition of phototrophy: adaptive strategies of hosting endosymbionts and organelles. *Photosynthesis Research*, 107, 117–132.

434 Johnson, M. D., Tengs, T., Oldach, D. & Stoecker, D. K. (2006). Sequestration, performance, and functional control of cryptophyte plastids in the ciliate *Myrionecta rubra* 436 (Ciliophora). *Journal of Phycology*, 42, 1235–1246.

Keeling, P. J., McCutcheon, J. P. & Doolittle, W. F. (2015). Symbiosis becoming per-438 manent: Survival of the luckiest. *Proceedings of the National Academy of Sciences of the United States of America*, 112, 10101–10103.

Lessard, E. J. & Murrell, M. C. (1996). Distribution, abundance and size composition of heterotrophic dinoflagellates and ciliates in the Sargasso Sea near Bermuda. *Deep Sea Research Part I: Oceanographic Research Papers*, 43, 1045–1065.

Löder, M. G. J., Meunier, C., Wiltshire, K. H., Boersma, M. & Aberle, N. (2011). The role of ciliates, heterotrophic dinoflagellates and copepods in structuring spring plankton communities at Helgoland Roads, North Sea. *Marine Biology*, 158, 1551–1580.

McGill, B. J., Enquist, B. J., Weiher, E. & Westoby, M. (2006). Rebuilding community ecology from functional traits. *Trends in Ecology & Evolution*, 21, 178–185.

McManus, G. B., Schoener, D. M. & Haberlandt, K. (2012). Chloroplast symbiosis in a marine ciliate: ecophysiology and the risks and rewards of hosting foreign organelles. *Frontiers in Microbiology*, 3, 1–9.

Mitra, A. & Flynn, K. J. (2010). Modelling mixotrophy in harmful algal blooms: More or less the sum of the parts? *Journal of Marine Systems*, 83, 158–169.

Mitra, A., Flynn, K. J., Burkholder, J. M., Berge, T., Calbet, A., Raven, J. A., Graneli, E., Glibert, P. M., Hansen, P. J., Stoecker, D. K., Thingstad, T. F., Tillmann, U., Våge, S., Wilken, S. & Zubkov, M. V. (2013). The role of mixotrophic protists in the biological carbon pump. *Biogeosciences Discussion*, 10, 13535–13562.

Moeller, H. V., Johnson, M. D. & Falkowski, P. G. (2011). Photoacclimation in the phototrophic marine ciliate *Mesodinium rubrum* (Ciliophora). *Journal of Phycology*, 47, 324–332.

Muggeo, V. M. R. (2003). Estimating regression models with unknown break-points. *Statistics in Medicine*, 22, 3055–3071.

Nielsen, L. T., Krock, B. & Hansen, P. J. (2012). Effects of light and food availability on toxin production, growth and photosynthesis in Dinophysis acuminata. *Marine Ecology Progress Series*, 471, 37–50.

Nielsen, T. G. & Kicrboe, T. (1994). Regulation of zooplankton biomass and production in a temperate, coastal ecosystem. 2. Ciliates. *Limnology and Oceanography*, 39, 508–519.

Ochman, H., Lawrence, J. G. & Groisman, E. A. (2000). Lateral gene transfer and the nature of bacterial innovation. *Nature*, 405, 299–304.

Park, M. G., Kim, M. & Kim, S. (2014). The acquisition of plastids/phototrophy in heterotrophic dinoflagellates. *Acta Protozoologica*.

Polis, G. A. & Holt, R. D. (1992). Intraguild predation: The dynamics of complex trophic interactions. *Trends in Ecology & Evolution*, 7, 151–154.

R Core Team (2014). *R: A Language and Environment for Statistical Computing*. R Foundation for Statistical Computing, Vienna, Austria. URL `http://www.R-project.org/`.

Ribera d'Alcala, M., Conversano, F., Corato, F., Licandro, P., Mangoni, O., Marino, D., Mazzocchi, M. G., Modigh, M., Montresor, M., Nardella, M., Saggiomo, V., Sarno, D. & Zingone, A. (2004). Seasonal patterns in plankton communities in a pluriannual time series at a coastal Mediterranean site (Gulf of Naples): an attempt to discern recurrences and trends. *Scientia Marina*, 68, 65–83.

Riisgaard, K. & Hansen, P. J. (2009). Role of food uptake for photosynthesis, growth and survival of the mixotrophic dinoflagellate Dinophysis acuminata. *Marine Ecology Progress Series*, 381, 51–62.

Rosenzweig, M. L. (1971). Paradox of Enrichment: Destabilization of Exploitation Ecosystems in Ecological Time. *Science*, 171, 385–387.

Sagan, L. (1967). On the origin of mitosing cells. *Journal of Theoretical Biology*, 14, 255–274.

Schoener, D. M. & McManus, G. B. (2012). Plastid retention, use, and replacement in a kleptoplastidic ciliate. *Aquatic Microbial Ecology*, 67, 177–187.

Skovgaard, A. (1998). Role of chloroplast retention in a marine dinoflagellate. *Aquatic Microbial Ecology*, 15, 293–301.

Smith, M. & Hansen, P. (2007). Interaction between Mesodinium rubrum and its prey: importance of prey concentration, irradiance and pH. *Marine Ecology Progress Series*, 1–10.

Stickney, H. L., Hood, R. R. & Stoecker, D. K. (1999). The impact of mixotrophy on planktonic marine ecosystems. *Ecological Modelling*, 125, 203–230.

Stoecker, D. K., Johnson, M. D., deVargas, C. & Not, F. (2009). Acquired phototrophy in aquatic protists. *Aquatic Microbial Ecology*, 57, 279–310.

Stoecker, D. K., Michaels, A. E. & Davis, L. H. (1987). Large proportion of marine planktonic ciliates found to contain functional chloroplasts. *Nature*, 326.

Stoecker, D. K., Silver, M. W., Michaels, A. E. & Davis, L. H. (1988). Obligate mixotrophy inLaboea strobila, a ciliate which retains chloroplasts. *Marine Biology*, 99, 415–423.

Stoecker, D. K., Taniguchi, A. & Michaels, A. E. (1989). Abundance of autotrophic, mixotrophic and heterotrophic planktonic ciliates in shelf and slope waters. *Marine Ecology Progress Series*, 50, 241–254.

Strom, S. L. (2001). Light-aided digestion, grazing and growth in herbivorous protists. *Aquatic Microbial Ecology*, 23, 253–261.

Tilman, D. (1977). Resource competition between plankton algae: an experimental and theoretical approach. *Ecology*, 58, 338–348.

van den Hoff, J. & Bell, E. (2015). The ciliate *Mesodinium rubrum* and its cryptophyte prey in Antarctic aquatic environments. *Polar biology*, 38, 1305–1310.

Yih, W., Kim, H. S., Myung, G., Park, J. W., Du Yoo, Y. & Jeong, H. J. (2013). The red-tide ciliate *Mesodinium rubrum* in Korean coastal waters. *Harmful Algae*, 30, S53–S61.

Figures

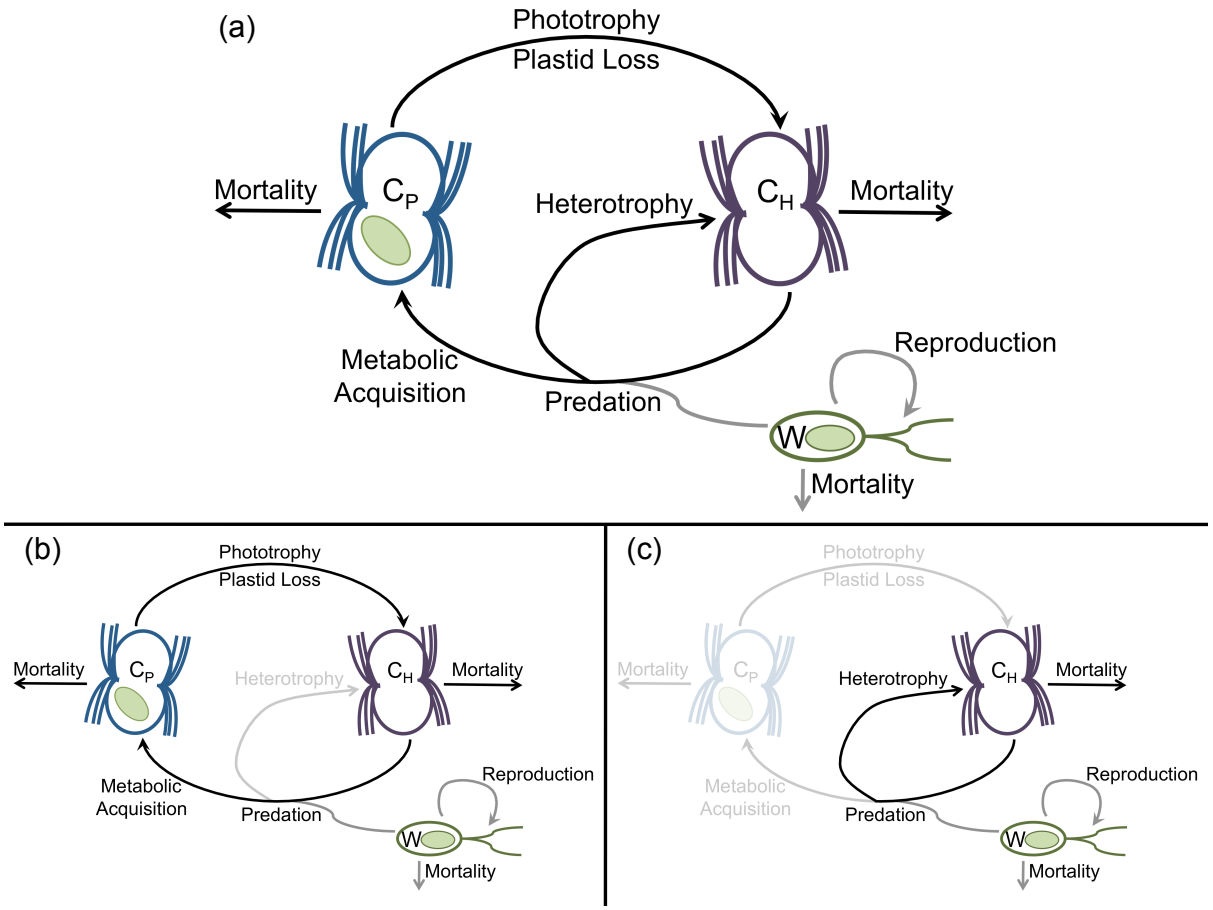

Figure 1: Intraguild acquired phototrophy. Panel a: Species W is a chloroplast-bearing phytoplankter that grows and reproduces through photosynthesis. Species C, the consumer, exists in two states: as a heterotroph (C_H) which predates W, and as a phototroph (C_P). The transition from C_H to C_P is mediated by predation events, in which prey are either consumed for heterotrophic growth, or processed to acquire photosynthetic machinery. C_P cells eventually lose their plastids and return to the heterotrophic state. We assume that C cannot independently replicate photosynthetic machinery; thus, photosynthetic growth by C_P yields new C_H cells which must re-acquire photosynthesis through a predation event. Panels b and c show strict acquired phototrophy and strict heterotrophy cases, respectively. Cell diagrams are modeled after the shapes of cryptophyte algae (W) and the ciliate *Mesodinium* (C). The *Mesodinium* genus includes both strict phototroph (e.g., *Mesodinium rubrum*) and near-strict heterotroph (e.g., *Mesodinium pulex*) members (Hansen *et al.*, 2013).

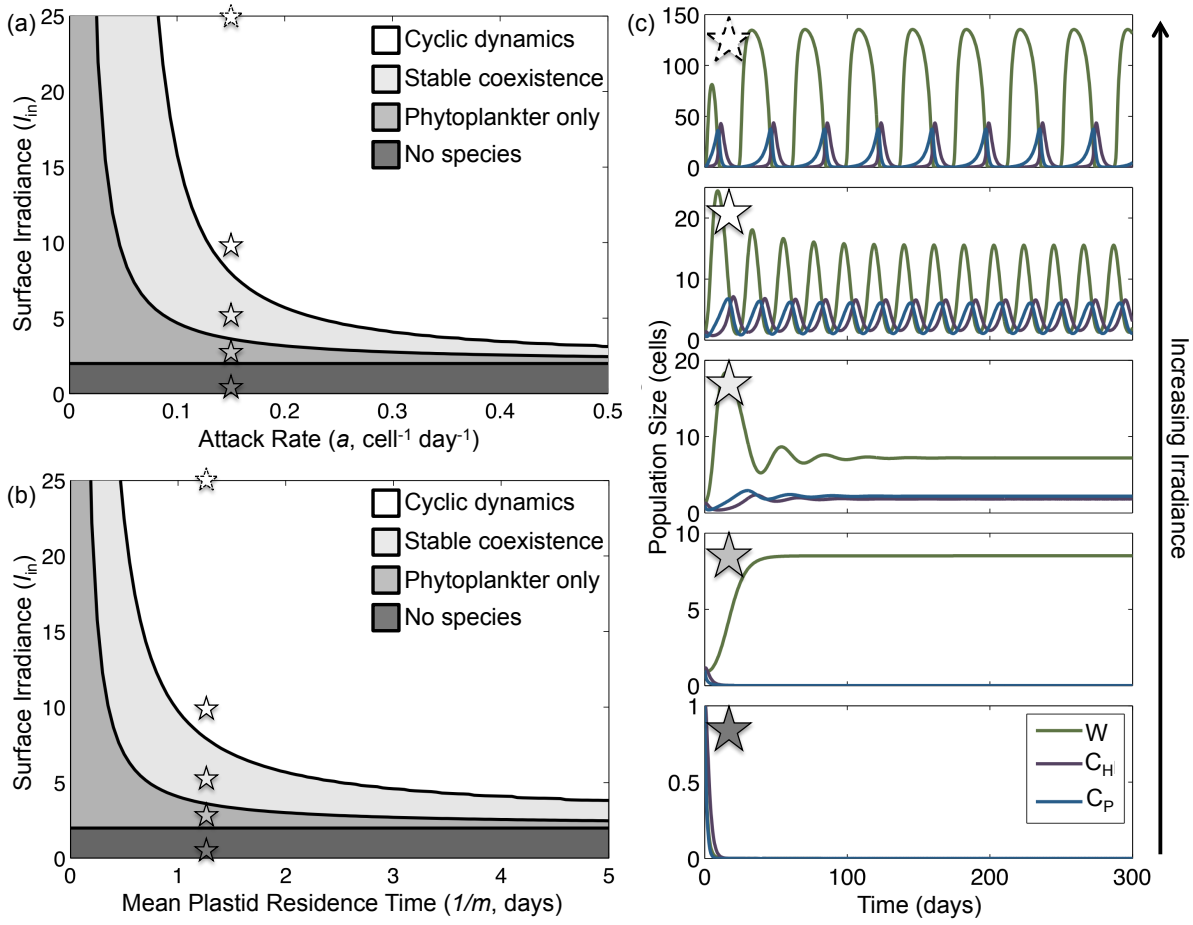

Figure 2: Dependence of model dynamics on habitat productivity (irradiance) and the strength of species interaction (attack rate, panel a; $m = 0.8$, other parameter values given in Table 1) and acquired metabolism persistence (panel b; $a = 0.15$, other parameter values given in Table 1) for a strict acquired phototroph ($f = 1$). Once irradiance exceeds the compensation point (I_C) for the phototroph W, that species can persist (boundary between dark gray and medium gray area). Intensification of either irradiance or attack rate, or a longer mean lifetime for the acquired plastid, allows for the persistence of the acquired phototroph C (medium gray to light gray boundary) and, eventually, causes a transition from stable equilibrium points to limit cycles (light gray to white boundary). Stars indicate parameter values corresponding to the sub-plots of representative time-series in panel c (for which $a = 0.15$, $m = 0.8$, and $f = 1$; other parameter values given in Table 1). As surface irradiance increases (moving from the bottom time-series panel upward), the equilibrium transitions from a stable point with no species present, to a stable point with only the phototroph present, to a stable point with coexistence of the phototroph and acquired phototroph, to to limit cycles of increasing amplitude and duration (note differences in y-axis scales).

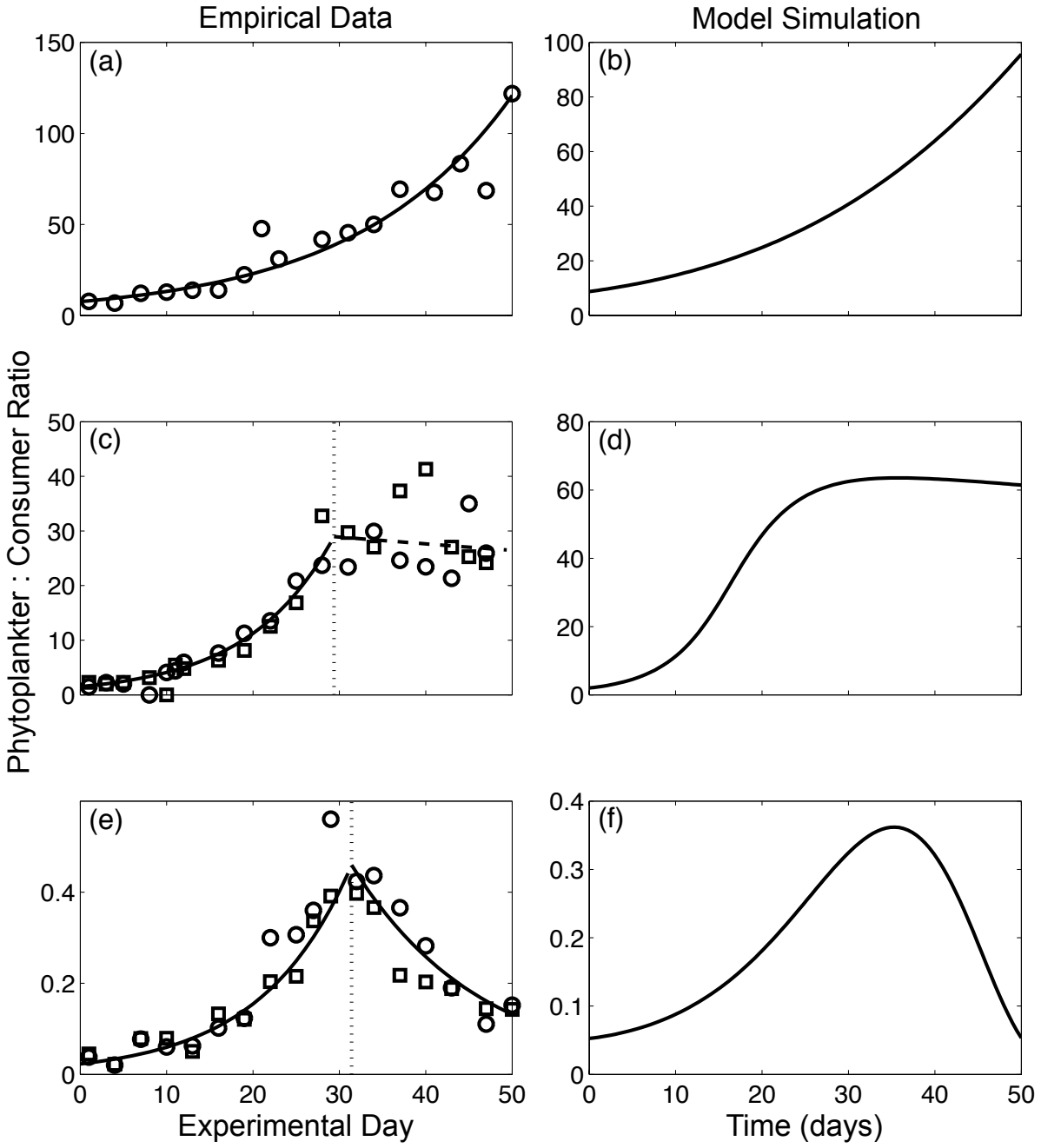

Figure 3: Dynamics produced by empirical manipulation of an acquired phototroph-prey system (left column) and model predictions (right column) are qualitatively similar. For panels a, c, and e, points represent ratios calculated from cell density measurements (shape indicates replicate). Solid lines show best-fit model predictions; dashed lines show non-significant slopes; dotted lines indicate breakpoints, where applicable. At low light (panels a-b), only the prey grows; at medium light (panels c-d), acquired phototroph and prey stably coexist; and at high light (panels e-f), populations exhibit boom-bust cycles. Parameters used for model simulation are listed in Table 1.

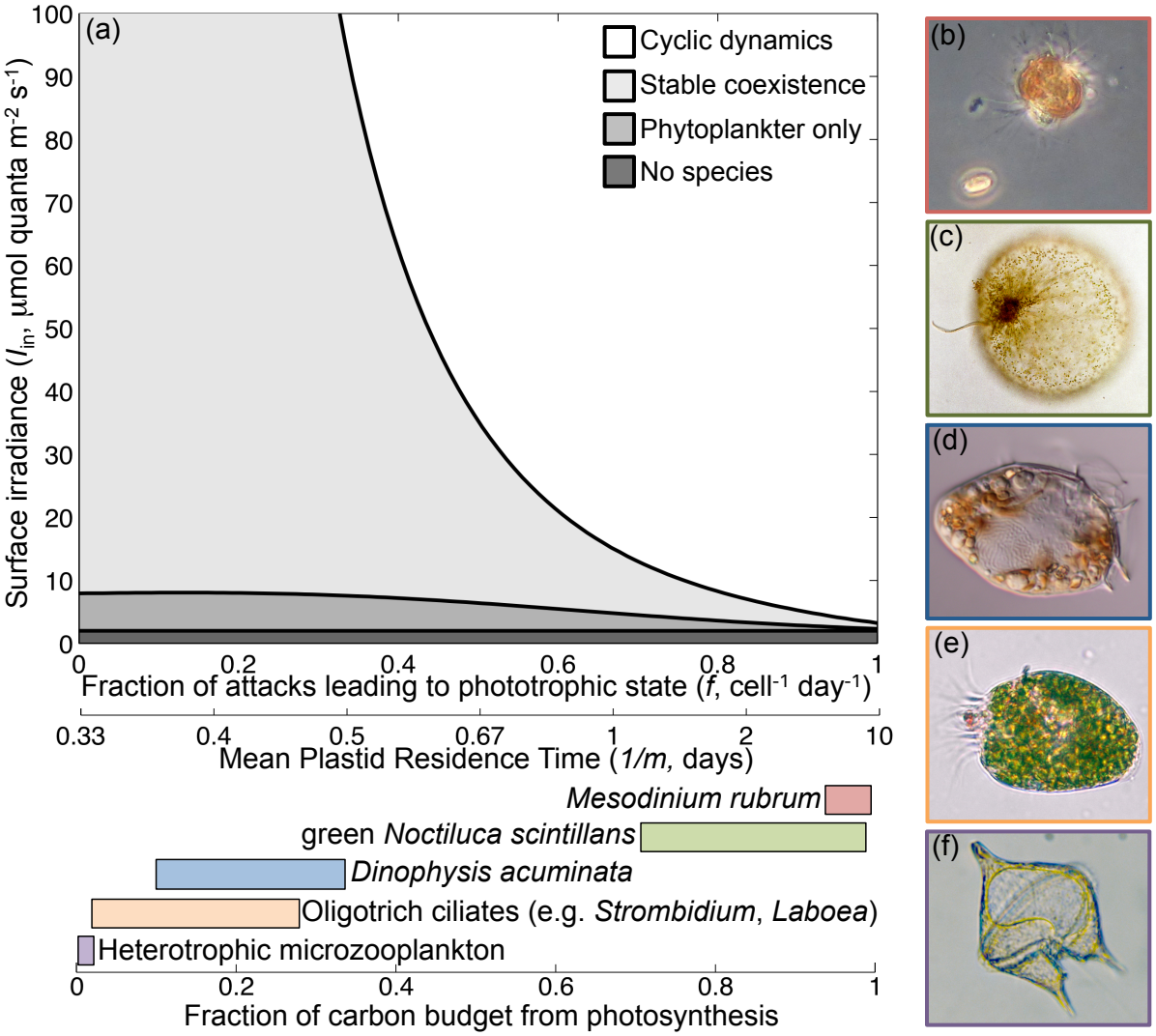

Figure 4: Dependence of model dynamics on the consumer's reliance on acquired phototrophy. Our literature survey revealed that acquired phototrophs range from strict acquired phototrophy to mixotrophy. Panel a: Our model codified this spectrum of dependence as the probability of retaining a plastid following a predation event, and the lifetime of that plastid once acquired. The more strict the consumer's reliance on acquired phototrophy, the lower the light threshold at which the community exhibits cyclic dynamics (Parameters as in Table 1; $a = 0.15$). Colored bars below panel a give examples of marine mesozooplankton species that fall along this acquired phototrophy dependence axis (published estimates of percent carbon budget from photosynthesis are used as a proxy for f). Empirical examples include: *Mesodinium rubrum* (Panel c, larger red cell, pictured with *Geminigera cryophila*, small cell in lower left, photo by H.V. Moeller), a bloom-forming ciliate (Hansen *et al.*, 2013); green *Noctiluca scintillans* (Panel d, courtesy of P.J. Hansen), a bloom-forming dinoflagellate (Hansen *et al.*, 2004); *Dinophysis acuminata* (Panel e, courtesy of L.T. Nielsen), a dinoflagellate that is known to cause diarrheic shellfish poisoning (Nielsen *et al.*, 2012; Riisgaard & Hansen, 2009); oligotrich ciliates (e.g. *Strombidium sp.*, Panel f, courtesy of G. McManus), which temporarily retain prey plastids (Stoecker *et al.*, 1988, 2009; McManus *et al.*, 2012); and pure heterotrophs (e.g. *Protoperidinium* sp., Panel g, photo by M.D. Johnson).

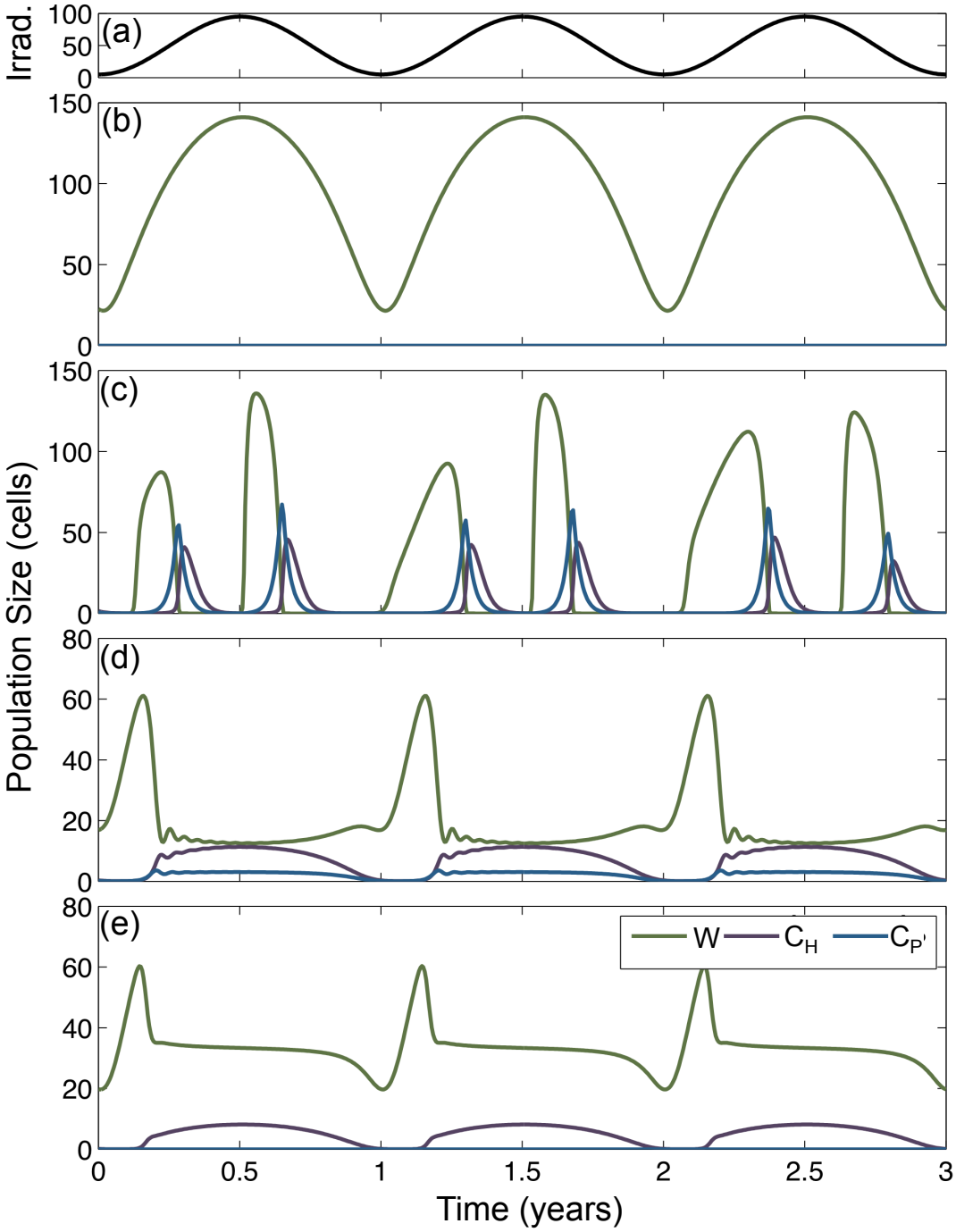

Figure 5: Annual cycles of phytoplankton (W) and consumer (C_H, heterotrophic state, and C_P, phototrophic state) populations. Population cycles are fundamentally driven by cyclic irradiance (i.e., seasonal variation in insolation; panel a) which, in the absence of higher trophic levels, produce seasonal phytoplankton blooms (panel b). When the consumer is present, community dynamics depend on its traits: strict acquired phototrophs (Panel c, $f = 1$, $m = 0.1$, e.g., *Mesodinium rubrum*) bloom sequentially following their phytoplankton prey; mixotrophic acquired phototrophs (Panel d, $f = 0.3$, $m = 2$, e.g., oligotrich ciliates) and pure heterotrophs (Panel e, $f = 0$, $m = 10$, e.g., heterotrophic dinoflagellates) damp phytoplankton blooms (note difference in ordinate scales) and then track phytoplankton population abundance. Model parameters are listed in Table 1.

Supplementary Table and Figures

Table S1: Refined model fit parameters allow for prey photoacclimation through variation in H_W with light intensity.

Parameter	Low Light	Intermediate Light	High Light
I_{in}	0.5	5	50
p_W	0.5	0.5	0.5
p_P	0.2	0.2	0.2
k_W	0.0001	0.0001	0.0001
k_H	0.000005	0.000005	0.000005
k_P	0.000015	0.000015	0.000015
H_W	0.5	2	4
H_P	10	10	10
l_W	0.2	0.2	0.2
l_H	0.03	0.03	0.03
l_P	0.01	0.01	0.01
a	0.000026	0.000026	0.000026
f	1	1	1
m	0.1	0.1	0.1

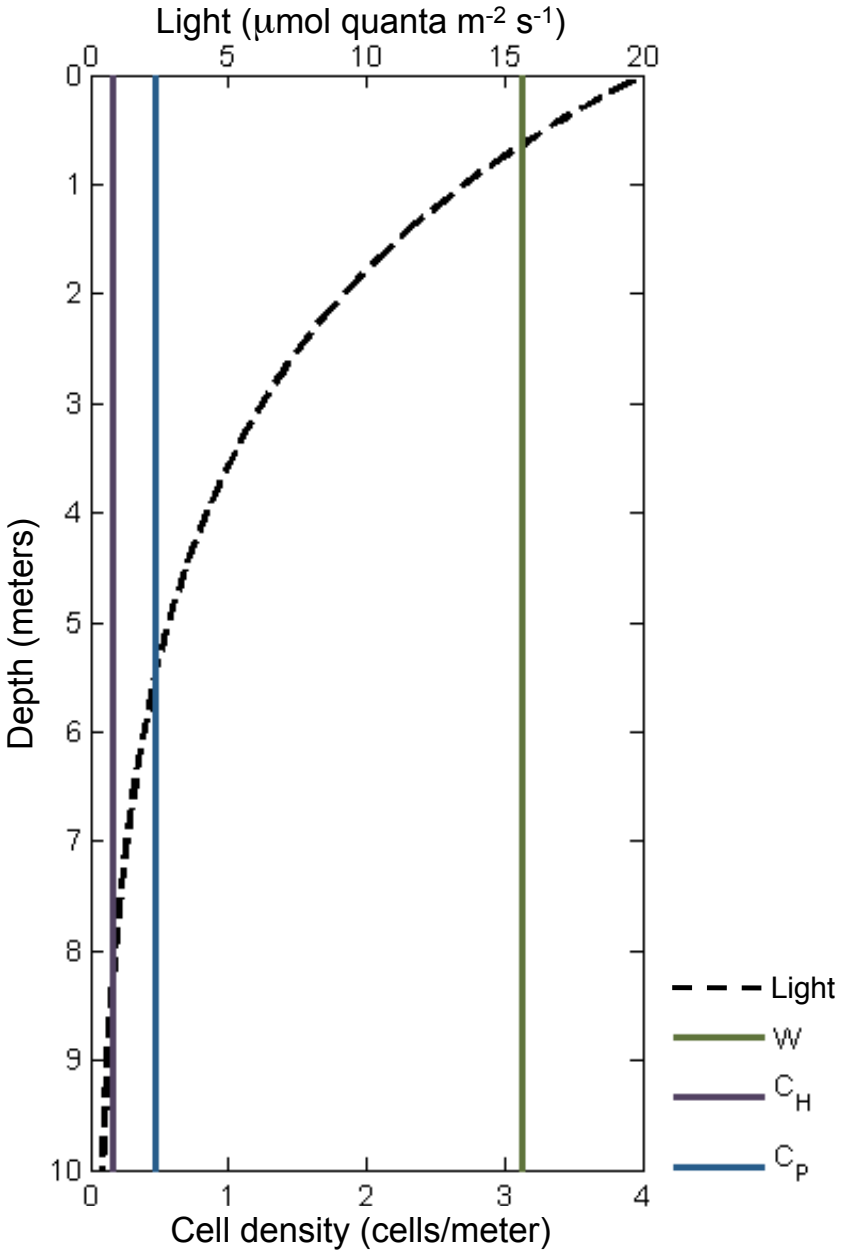

Figure S1: Example depth profile. Light (dashed black line) declines exponentially with depth due to absorption by the phytoplankter W and the consumer C. The water column is well-mixed, so cell densities are constant throughout the water column.

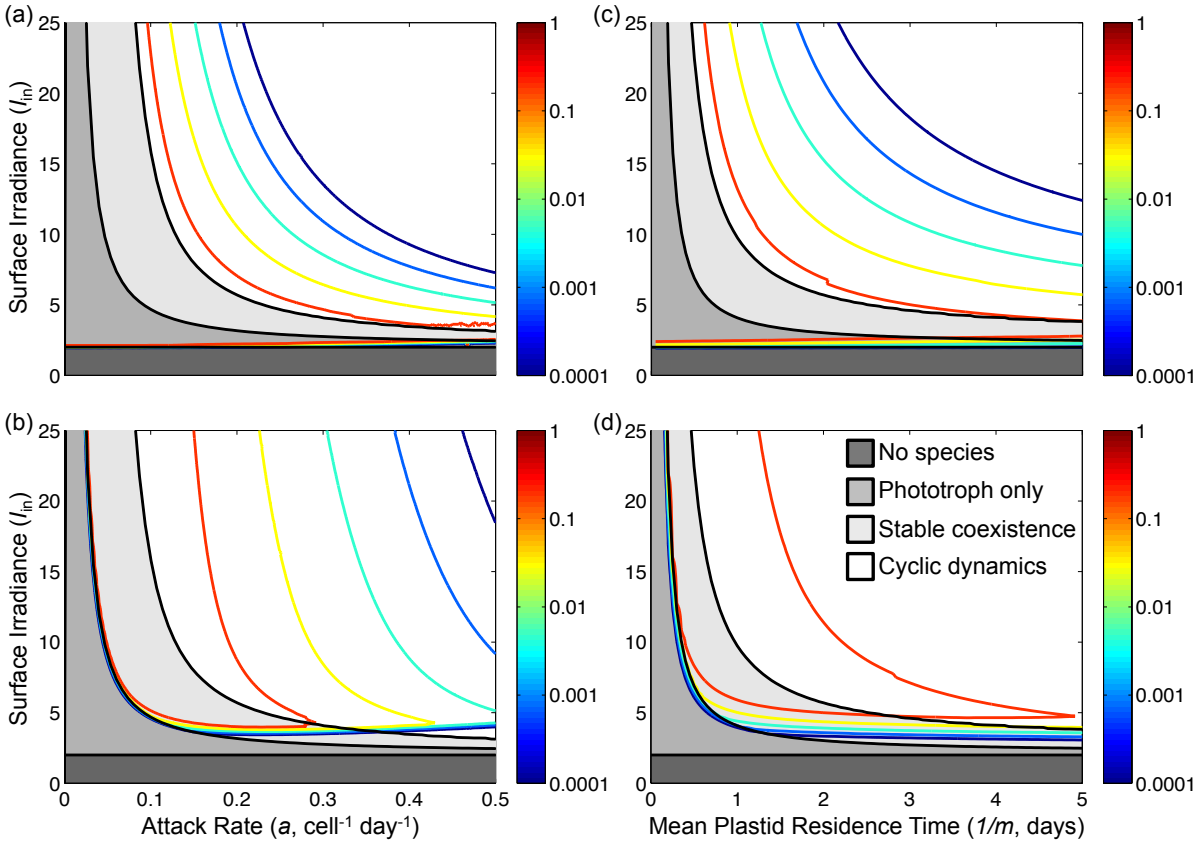

Figure S2: Minimum population sizes for the phytoplankter prey W (top row) and the consumer (bottom row; summed across both states, $C_P + C_H$) as a function of incoming irradiance and attack rate (panels a,b) or mean plastid retention time (panels c,d). Grayscale areas indicate the corresponding asymptotic dynamics (as in Figure 2).

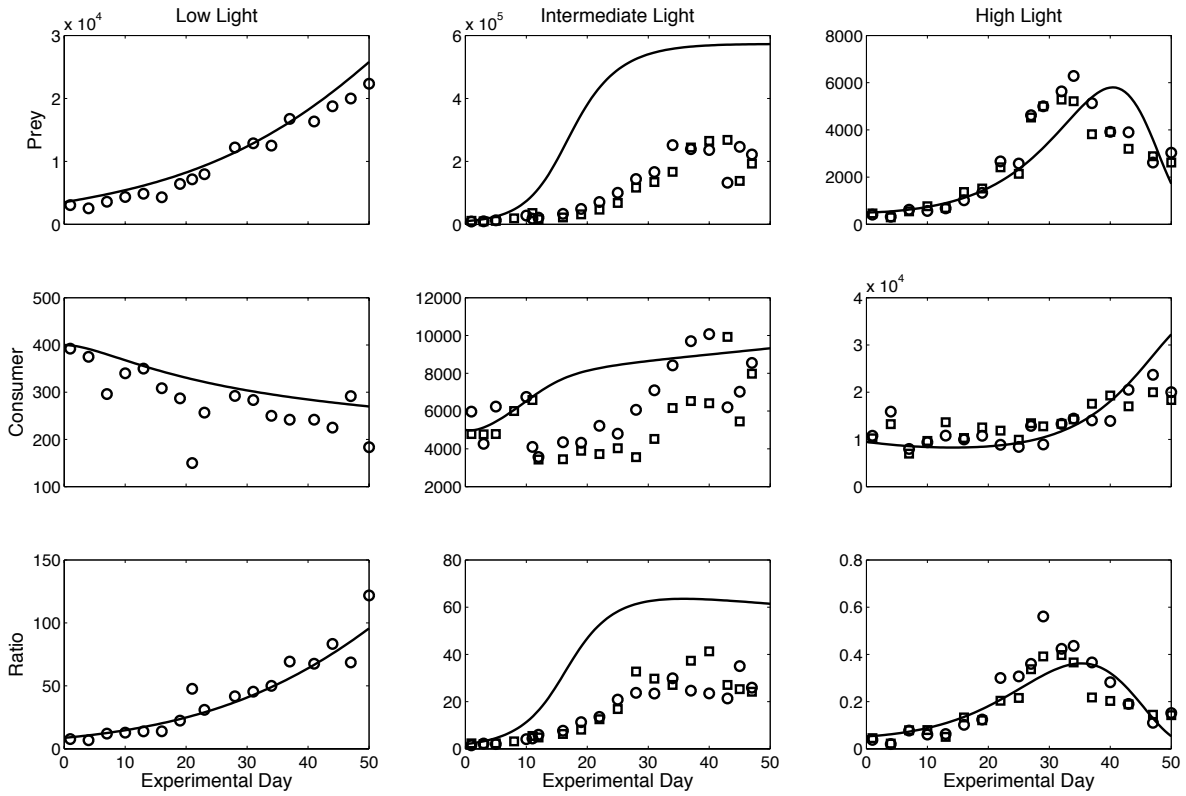

Figure S3: Full comparison of mathematical and laboratory models. Experimental data (points; replicates indicated by different shapes) are plotted alongside numerical simulations (solid lines) for phytoplankter prey (top row) and consumer (middle row) population sizes, and their ratio (bottom row). From left to right, columns show data for low, intermediate, and high light levels.

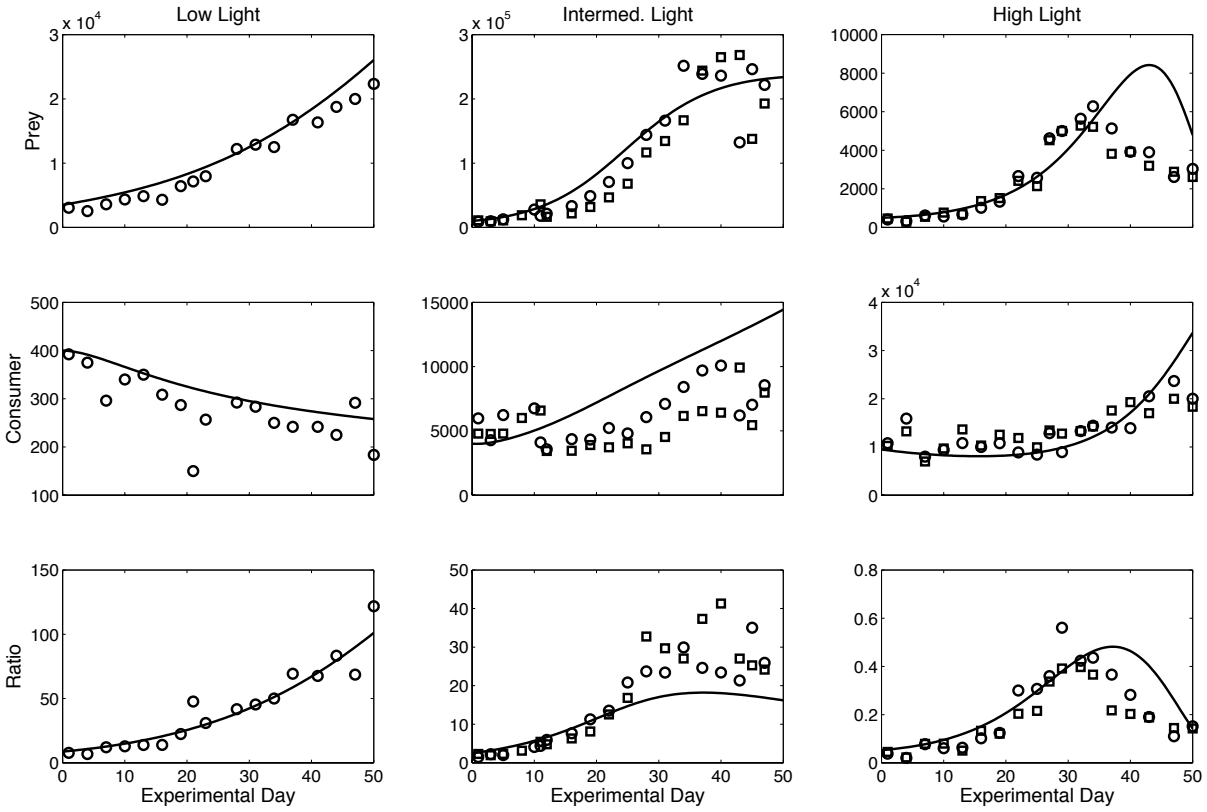

Figure S4: We performed a secondary model-fitting exercise in which we allowed for photoacclimation in the phytoplankter prey by varying the half-saturation light levels H_W to vary with increasing surface irradiance (see Table S1 for parameters). This improved the quantitative match between mathematical (solid lines) and laboratory (points; replicates indicated by different shapes) models for phytoplankter population sizes (top row), consumer population sizes (middle row), and the phytoplankter-consumer ratio (bottom row).

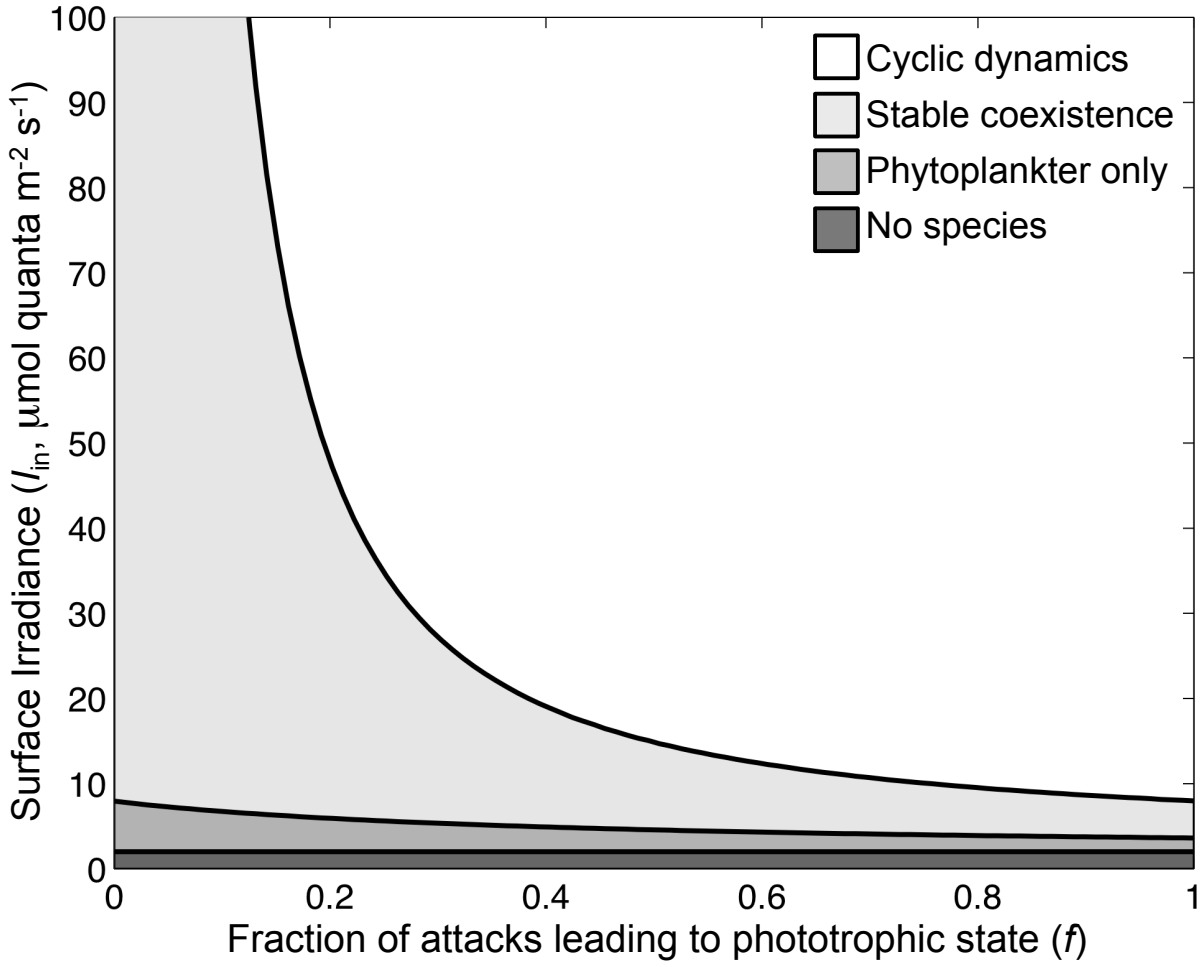

Figure S5: Effect of dependence on phototrophy on model dynamics. Strict acquired phototrophs ($f = 1$, right side of the abscissa) exhibit intrinsic limit cycles at lower irradiances than strict heterotrophs ($f = 0$, left side of the abscissa).